

# Spin nematics next to spin singlets

Yuto Yokoyama and Chisa Hotta<sup>1,\*</sup>

<sup>1</sup>*Department of Basic Science, University of Tokyo, 3-8-1 Komaba, Meguro, Tokyo 153-8902, Japan*  
(Dated: March 4, 2022)

We provide a route to generate nematic order in a spin-1/2 system. Unlike the well-known magnon-binding mechanism, our spin nematics requires neither the frustration effect nor a spin polarization in a high field or in the vicinity of a ferromagnet, but instead appears next to the spin singlet phase. We start from a state consisting of a quantum spin-1/2 singlet dimer placed on each site of a triangular lattice, and show that inter-dimer ring exchange interactions efficiently dope the SU(2) triplets that itinerate and interact, easily driving a stable singlet state to either Bose Einstein condensates or a triplet crystal, some hosting a spin nematic order. A variety of roles the ring exchange serves include the generation of a bilinear-biquadratic interaction between nearby triplets, which is responsible for the emergent nematic order separated from the singlet phase by a first order transition.

PACS numbers: 73.43.Nq, 75.10.Pq, 75.50.Ee, 75.40.Cx

*Introduction.*— Challenges in modern magnetism have been to clarify the role of the intrinsic quantum effect in exotic phases of matter. Spin-1/2 liquids<sup>1,2</sup> that do not break any symmetry are characterized by the long range entanglement of their wave functions. Some phases break the symmetry quantum mechanically by forming the smallest entangled unit; a valence bond crystal is the long range order of a spin-1/2 singlet breaking translational symmetry<sup>3</sup>, and *spin nematics* is the SU(2)-symmetry-broken order of the quadrupole moment based on spin-1 pairs<sup>4,5</sup>. The latter phase is our focus, and is established in a spin-1 bilinear-biquadratic Hamiltonian on square<sup>6–10</sup> and triangular lattices<sup>11–13</sup>; they appear whenever the biquadratic interaction  $(\mathcal{S}_i \cdot \mathcal{S}_j)^2$ , overwhelms the bilinear (Heisenberg) term where  $\mathcal{S}_i$  is the spin-1 operator. In fact, to entangle a pair of spin-1, one needs to exchange  $(\mathcal{S}_i^z, \mathcal{S}_j^z) = (+1, -1)$  with  $(-1, +1)$  by the biquadratic term, such that the spin-1/2 singlets are formed by a Heisenberg exchange, flipping  $(+1/2, -1/2)$  spins to  $(-1/2, +1/2)$ . Unfortunately, the spin-1 biquadratic interaction is usually much weaker than the bilinear term which makes the nematic phase as elusive as spin liquids.

Moreover, spin-1 is not the basic magnetic unit in condensed matter, since it appears only as a triplet pair of spin-1/2's of localized electrons. When the spin-1 is broken into pieces of 1/2, higher order exchanges among spin-1/2's are required to realize the spin nematics. The simplest one is the four-body ring exchange interaction. When this interaction is applied to the polarized spin-1/2 magnets in a strong magnetic field or near the ferromagnetically ordered phases, a nematic order indeed appears<sup>14,15</sup>, providing a good reference for a solid <sup>3</sup>He<sup>16,17</sup>. There, the ring exchange was ascribed a role to enhance quantum fluctuation among competing magnetic orders<sup>15,18</sup>. Besides, this interaction generates a gapped spin liquid in a spin-1/2 triangular lattice antiferromagnet<sup>19–21</sup>. The magnitude of ring exchange is enhanced near the Mott transition<sup>22</sup>, which may explain the origin of the spin liquid triangular lat-

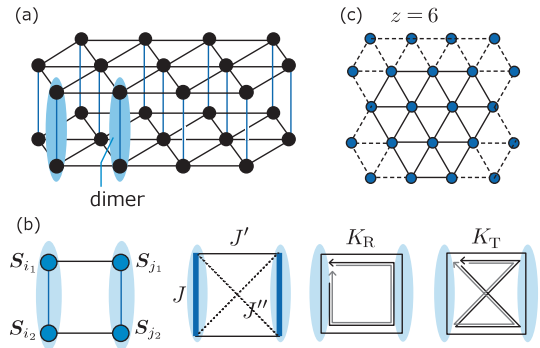


FIG. 1. (color online) (a) Triangular lattice based on  $S = 1/2$  dimers. Right panel is the top view of the lattice, and the  $N = 12$  sites used for the diagonalization. (b) Inter-site interactions: Antiferromagnetic Heisenberg exchange  $J, J'$ , and  $J''$ , four-body ring exchange ( $K_R$ ) and twisted ring exchange ( $K_T$ ). (c) Example of the operation of  $K_R$  and  $K_T$  to the  $S^z = \pm 1$  dimers. Spin-1/2's are permuted cyclically and become  $S^z = 0$  and  $\mp 1$  states by  $K_R$  and  $K_T$ , respectively. The latter contribute to the spin-1 biquadratic term.

tice Mott insulator<sup>23</sup> possibly realized in the organic  $\kappa$ -ET<sub>2</sub>Cu<sub>2</sub>(CN)<sub>3</sub><sup>24</sup>. The ring exchange further supports the anomalous thermal magnon Hall transport in a kagome ferromagnet<sup>25</sup>. Despite such rich physics relevant to the ring exchange, a clear-cut and systematic understanding of its role is still lacking.

This Rapid Communication shows how the ring exchange serves to yield a variety of quantum phases. We consider spin-1/2 antiferromagnetically coupled dimers forming a triangular lattice. When the ring exchange interactions are transformed into a bosonic language, they simultaneously play different roles: chemical potential, hoppings, and repulsive/attractive interactions. Particularly, the one called *twisted ring exchange* flips the  $\mathcal{S}_i$  pairs up side down, and contributes to the bilinear-biquadratic interactions. We obtain a rich phase diagram in the bulk limit that hosts Bose Einstein conden-

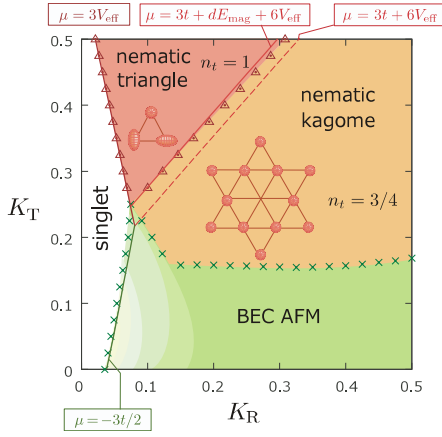


FIG. 2. (color online) Phase diagram of Eq.(1) on the plane of  $K_R$  and  $K_T$ , with  $J = 1$ ,  $J'' = 0$  and  $J' = 2K_R$ . The triangle and cross symbols indicate the first and second order transitions, respectively, obtained by analysis of exact diagonalization with  $N = 12(24)$  spins. Solid lines are the analytical phase boundaries. By increasing  $J'$  and  $J''$ , the nematic phase is stabilized toward smaller  $K_R$  and  $K_T$  (see Supplementally Material).

sate(BEC) of  $SU(2)$  bosons and nematic orders of triangular and kagome geometries.

*Model and Phase Diagram.*— Each lattice site consists of a pair of quantum spin-1/2 coupled by the antiferromagnetic Heisenberg interaction,  $J$ , as shown in Fig.1(a). When we consider only  $J(=1)$ , the ground state is an exact product state of singlets with energy  $E_0 = -NJ/4$ . By introducing the inter-dimer interactions, our Hamiltonian is given as,

$$\mathcal{H} = \sum_{i=1}^N J \mathbf{S}_{i_1} \cdot \mathbf{S}_{i_2} + \sum_{\langle i,j \rangle, \gamma=1,2} (J' \mathbf{S}_{i_\gamma} \cdot \mathbf{S}_{j_\gamma} + J'' \mathbf{S}_{i_\gamma} \cdot \mathbf{S}_{j_{\gamma'}}) + \sum_{\mathcal{C}} K_C \left( (P_4 + P_4^{-1}) - \frac{9}{5} \sum_{(i_\gamma, j_{\gamma'}) \in \mathcal{C}} \mathbf{S}_{i_\gamma} \cdot \mathbf{S}_{j_{\gamma'}} \right) \quad (1)$$

where  $\mathbf{S}_{i_1}, \mathbf{S}_{i_2}$  are the spin-1/2 operators forming the  $i$ -th dimer,  $J'$  and  $J''$  are the Heisenberg (bilinear) exchanges, and  $K_C$  denotes the four-body exchange (see Fig.1(b)). Along the two different closed loops  $\mathcal{C} = R$  and  $T$ , the four spins permute both clockwise ( $P_4$ ) and anticlockwise ( $P_4^{-1}$ ), which we call the ring exchange (R) and twisted ring exchange (T)<sup>26</sup>, e.g. as those shown in Fig.1(c). The last two-body term appears when deriving the four-body interactions by the perturbation from the Hubbard model at half-filling<sup>27–29</sup>.

Due to the ring exchange terms, a variety of phases emerges as shown in Fig.2; when  $K_T$  is small,  $K_R$  drives the system to the BEC of triplets. At larger  $K_T$ , the nematic phases become dominant. Here, we stress that all the  $\mathcal{S}_i^z = 1, 0, -1$  component of triplets equivalently join this BEC, which is thus *different from a magnon BEC* (carrying a net magnetic moment) that typically appears

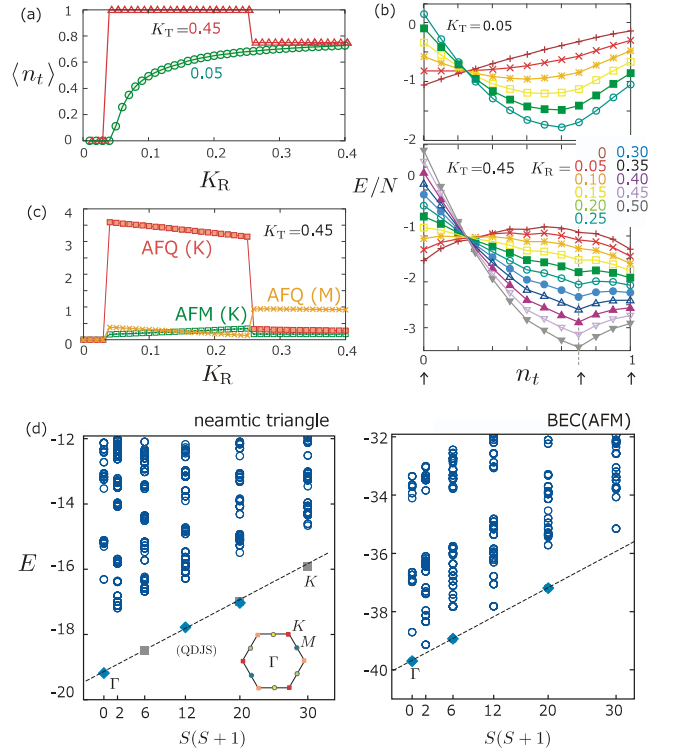


FIG. 3. (color online) (a) Density of triplets,  $\langle n_t \rangle$  as a function of  $K_R$ . In BEC,  $\langle n_t \rangle$  changes gradually. A nematic triangle and kagome have exactly  $\langle n_t \rangle = 1$  and  $3/4$ , respectively. (b) Exact diagonalization energy per site  $E/N$  of Eq.(1) as a function of triplet density,  $n_t$ , at  $K_T = 0.05, 0.45$  and  $K_R = 0 \sim 0.5$ . (Upper panel) BEC phase with no anomaly. (Lower panel) Dips at  $n_t = 0, 3/4, 1$  indicate the three other stable phases in Fig.2, and the first order transitions between them. (c) Structural factor of  $\langle Q_i \cdot Q_j \rangle$  at the  $K$  and  $M$ -points on the Brillouin zone boundary, together with the ones for  $\langle \mathcal{S}_i \cdot \mathcal{S}_j \rangle$ , characterizing  $120^\circ$  magnetic ordering (AFM). (d) Tower of states in the nematic triangular ( $K_R = 0.1, K_T = 0.45$ ) and BEC-AFM ( $K_R = 0.5, K_T = 0$ ) phases.

in spin singlet systems by the magnetic field<sup>30–33</sup>. The spin nematics in a quantum spin-1/2 system known so far is based on a bound state of magnons created by the frustration effect, in a strong magnetic field or near the fully polarized ferromagnetic phase<sup>14,34,35</sup>. Our spin nematics *does not require such frustration*, and the overall feature of the phase diagram applies to square, honeycomb, and ladder systems as well<sup>36</sup>.

*Bosonic representation.*— To understand the nature of the phase diagram, it is convenient to transform the basis in units of dimers rather than of spin-1/2's<sup>37,38</sup>. Each dimer hosts either a singlet ( $\mathcal{S}_i = \mathbf{S}_{i_1} + \mathbf{S}_{i_2} = 0$ ) or one of the triplets ( $\mathcal{S}_i = 1, \mathcal{S}_i^z = 1, 0, -1$ ). Therefore, by regarding the singlet product state as a vacuum, we introduce a bosonic operator,  $b_{i,\alpha}^\dagger/b_{i,\alpha}$  with  $\alpha = 1, 0, -1$ , which creates/annihilates a triplet with  $\mathcal{S}_i^z = 1, 0, -1$  on

an  $i$ -th dimer. Equation (1) is *exactly* transformed to  $\mathcal{H} = \mathcal{H}_{tV} + \mathcal{H}_{\text{mag}} + \mathcal{H}_{\text{pair}}$  with

$$\begin{aligned}\mathcal{H}_{tV} &= \sum_{\langle i,j \rangle, \alpha} (t(b_{i,\alpha}^\dagger b_{j,\alpha} + b_{j,\alpha}^\dagger b_{i,\alpha}) + V n_i n_j) - \sum_{i=1}^N \mu n_i \\ \mathcal{H}_{\text{mag}} &= \sum_{\langle i,j \rangle} \left( \mathcal{J}(\mathcal{S}_i \cdot \mathcal{S}_j) + \mathcal{B}(\mathcal{S}_i \cdot \mathcal{S}_j)^2 \right) n_i n_j \\ \mathcal{H}_{\text{pair}} &= \sum_{\langle i,j \rangle} P(b_{i,1}^\dagger b_{j,-1}^\dagger + b_{i,-1}^\dagger b_{j,1}^\dagger - b_{i,0}^\dagger b_{j,0}^\dagger) + \text{H.c.},\end{aligned}\quad (2)$$

where  $n_i = 0$  or 1 is the number operator of bosons under a hard core condition, and  $\mathcal{S}_i$  is the spin-1 operator on site- $i$  when it is occupied by a triplet, and fulfills  $\mathcal{S}_i^+ = b_{i,1}^\dagger b_{i,0} + b_{i,0}^\dagger b_{i,-1}$ ,  $\mathcal{S}_i^- = b_{i,0}^\dagger b_{i,1} + b_{i,-1}^\dagger b_{i,0}$ , and  $\mathcal{S}_i^z = b_{i,1}^\dagger b_{i,1} - b_{i,-1}^\dagger b_{i,-1}$ . The magnetic interactions,  $\mathcal{J}$  and  $\mathcal{B}$ , will be discussed shortly. The parameters are given as,

$$\mu = -J + \left( \frac{96}{5} K_R - \frac{24}{5} K_T \right), \quad (3)$$

$$t = \frac{1}{2}(J' - J'') + K_R, \quad (4)$$

$$V = 4(K_R - K_T), \quad (5)$$

$$P = \frac{1}{2}(J' - J'') - K_R. \quad (6)$$

In the present Rapid Communication, we take  $J' = 2K_R$  and  $J'' = 0$ , in order to keep  $P = 0$ , which allows for the exact evaluation of the phase boundaries, and the number of triplets is conserved. The role of  $P \neq 0$  is mainly to enhance  $\mathcal{B}$  and stabilize the nematic order (see Supplemental Material), while the physics itself is not influenced qualitatively.

As the chemical potential,  $\mu$ , gets lower with  $K_R$ , the bosons are doped to the vacuum (singlet). Meanwhile, there arises an interaction between doped bosons. Figure 3(a) shows how the expectation value of the triplet density,  $n_t \equiv \sum_i n_i / N$ , develops, where  $\langle n_t \rangle$  is the value that gives the minimum of total energy  $E$  among all different  $n_t$ -sectors in Fig.3(b). At  $K_R > K_T$ , the kinetic energy gain due to  $t$  favors doping the bosons, but the repulsive interaction  $V > 0$  does not, thus  $\langle n_t \rangle$  increases gradually due to their competition. Contrarily at  $K_R < K_T$ , the attractive  $V < 0$  helps  $\mu$  to dope triplets and there occurs a first order transition from the  $\langle n_t \rangle = 0$  to the  $\langle n_t \rangle = 1$  phase, which is also visible in the dip of energies at  $n_t = 0$  and 1 in Fig.3(b). Once all the sites are occupied by triplets, their spin-1's interact via  $\mathcal{H}_{\text{mag}}$ , which takes a well known form called the bilinear-biquadratic interaction, with  $\mathcal{B} = 2K_T$  and  $\mathcal{J} = (-K_R + 4K_T)/5 + (J' + J'')/2$ . In a triangular lattice, the spin-1 bilinear-biquadratic Hamiltonian is known to host a nematic long range order when  $\mathcal{B} > \mathcal{J}^{11,12}$ , and the equivalent condition,  $K_T > 3K_R/2$ , is actually fulfilled in our nematic triangular phase.

*Spin nematic order.*— The quadrupolar moment is the order parameter of the spin nematics and is described by a symmetric and traceless rank-2 tensor,  $Q_j^{\alpha\beta} = \mathcal{S}_j^\alpha \mathcal{S}_j^\beta +$

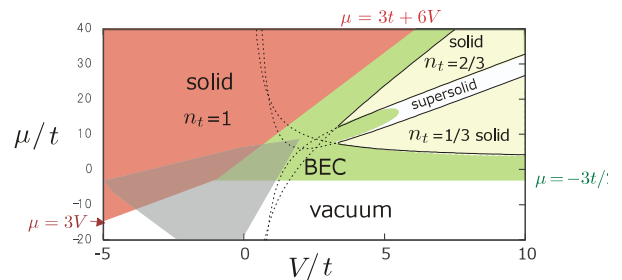


FIG. 4. (color online) Phase diagram of the hard core bosonic model  $\mathcal{H}_{tV}$  with  $t > 0$ . The boundaries are evaluated analytically (for details see Ref.43). The shaded area marks the parameter region realized in the phase diagram of Fig.2.

$\mathcal{S}_j^\beta \mathcal{S}_j^\alpha - 2\mathcal{S}(\mathcal{S} + 1)/3\delta_{\alpha\beta}$ . We examined its two point correlation whose structural factor takes a peak at the  $K$  and  $M$ -points at the Brillouin zone boundary, which are plotted as functions of  $K_R$  in Fig.3(c). A dominant peak at the  $K$ -point is consistent with the previously reported antiferro-quadrupolar ordering (AFQ) on the triangular lattice. The peak of the spin-spin correlation function at the  $K$ -point, characterizing the  $120^\circ$  antiferromagnetic (AFM) ordering is suppressed in these regions.

To further confirm the existence of nematic long range order, we show the energy spectrum at  $K_T = 0.5$  and  $K_R = 0.1$  in Fig. 3(d). There actually appears a tower of low-lying energy levels well separated from the other excitations<sup>39,40</sup>, and the symmetries of the quasidegenerate joint states (QDJS) belonging to different spin sectors follow those already known for the SU(2)-symmetry-broken spin nematics on a triangular lattice<sup>41</sup>. We also give the same analysis on the BEC phase, finding that the antiferromagnetic long range order expected for  $0 < \mathcal{B} < \mathcal{J}$  in this region is realized as well. Notice that this phase is different from the AFM of a localized spin-1 system since the triplets are not fully occupied ( $\langle n_t \rangle < 1$ ). The slopes of the two towers are almost equal, further confirming the well known scaling behavior,  $E_{\text{QDJS}} \propto S(S + 1)/N$ .

*Twisted ring exchange.*— We need to understand why the biquadratic  $\mathcal{B}$  in  $\mathcal{H}_{\text{mag}}$  (Eq.(2)) originates from the twisted ring exchange,  $K_T$ , and not from  $K_R$ . The spin-1 biquadratic term exchanges the up and down spin-1 pairs, changing  $\mathcal{S}_i^z$  by  $\pm 2$ , while the Heisenberg (bilinear) term flips  $\mathcal{S}_i^z$  only by the  $\pm 1$ . Figure 1(d) shows that when  $K_R$  is operated to the four spin-1/2's on a plaquette, they move cyclically, and transform the dimer spin  $(\mathcal{S}_i^z, \mathcal{S}_j^z) = (+1, -1)$  to  $(0, 0)$ . Whereas, if the path is twisted,  $K_T$  can move the two spin 1/2's on one dimer to the other dimer at once, and flip the dimer spin  $(+1, -1)$  to  $(-1, +1)$ , contributing to the biquadratic term.

The magnitude of  $K_T$  had been considered as small in a quantum spin system, as it originates from the fourth order perturbation in a Mott insulator<sup>28</sup>. According to our evaluation<sup>27</sup>, the on-site Coulomb interaction  $U$  against the inter-dimer transfer integral,  $t_{ij} = t'$  or  $t''$  should be

$U/t_{ij} \lesssim 7$  in order to have  $K_C/J \gtrsim 0.1$ , which is not too unrealistic. It is also shown that in the vicinity of the Mott transition,  $U/t \sim 8$ , the ring exchanges can be as large as  $J/4$ <sup>22</sup>. We further mention that  $P \neq 0$  works as an effective biquadratic term, thus a larger  $J' - J''$  will stabilize the nematic phase than the one found in Fig. 2. (see Supplementary Material).

*Instabilities.*— The phase boundaries of Fig.2 can be determined half-analytically by examining the energetics of the hard core bosonic model,  $\mathcal{H}_{tV}$ , in the bulk limit<sup>42</sup>. The phase diagram of  $\mathcal{H}_{tV}$  for  $t > 0$  is shown in Fig.4<sup>43</sup>. Similar to the case of  $t < 0$  studied in the context of cold atoms<sup>44–47</sup>, the 1/3- and 2/3-filled crystal phases appear at large  $V/t$ , and the supersolid phases in between. The other parts are divided into the vacuum, bosonic BEC, and a solid, and their boundaries are *exactly* determined; The onset of the BEC from the vacuum is given by the kinetic energy gain of a single boson,  $\mu = -3t/2$ . The first order transition line between the vacuum and the solid takes place at  $\mu = 3V$ , as the attractive interaction favors all the triplets to be doped at once by maximally gaining the energy  $3V < 0$ . Finally, the instability of the solid against the BEC is evaluated by the energy of a doped hole,  $-3t - 6V$ .

The shaded region in Fig.4 covers the parameter range of Fig.2. The onset of BEC mapped to our model is,  $111K_R - 24K_T = 5J$ , in good agreement with the one from the exact diagonalization. In regions with higher boson densities, the bosons interact magnetically, thus we need to take account of the effect of  $\mathcal{H}_{\text{mag}}$  terms on the energy of hard core bosons. For this purpose, we introduce an effective interaction including the corrections from the magnetic terms,  $V_{\text{eff}} = V + \langle \mathcal{J}(\mathcal{S}_i \cdot \mathcal{S}_j) + \mathcal{B}(\mathcal{S}_i \cdot \mathcal{S}_j)^2 \rangle$ , and evaluate its value by separately analyzing the spin-1 bilinear-biquadratic Heisenberg model. Originally, the upper left-half of the phase diagram,  $K_T > K_R$  was the region with an attractive interaction  $V < 0$ . However, this correction pushes the phase boundary upward, and the repulsive  $V_{\text{eff}} > 0$  region starts just below the triangular nematic phase. The boundary between the singlet and the nematic triangle is given by  $\mu = 3V_{\text{eff}}$ .

*Nematic kagome phase.*— There is another phase in the middle of the diagram with  $\langle n_t \rangle = 3/4$ , characterized by the peak of the AFQ order at three  $M$ -points (see Fig.3(c),(d)). The spatial structure of this quadrupole order expected is a kagome geometry that is realized by regularly depleting one quarter of the lattice sites of the triangular lattice. However, in a pure hard core bosonic model, there is no reason to favor such a kagome structure which is indeed absent in Fig.4. We thus reexamine the energy of the original Hamiltonian for all different  $n_t$  sectors in Fig. 3(b); there is a dip in the energy at  $\langle n_t \rangle = 3/4$ , which competes with  $\langle n_t \rangle = 1$  when  $K_T \gtrsim 0.3$ <sup>48</sup>. This is in sharp contrast to the smooth  $n_t$  dependence of  $E$  in the BEC region. The competition between the three discrete fillings gives the first order transitions. The energy dip at  $\langle n_t \rangle = 3/4$  comes solely from the magnetic

interaction,  $\langle \mathcal{H}_{\text{mag}} \rangle$ , and not from  $\langle \mathcal{H}_{tV} \rangle$  (Supplementary Material Fig. S2), to be more precise, by the contribution from  $\mathcal{B}(\mathcal{S}_i \cdot \mathcal{S}_j)^2 = \mathcal{B}/2(\langle Q_i \cdot Q_j \rangle - \langle \mathcal{S}_i \cdot \mathcal{S}_j \rangle) + \text{const.}$  This also suggests that the bosons remain BEC. We calculate the bond energy of the bilinear biquadratic Hamiltonian on a kagome lattice, and find that it is lower by  $dE_{\text{mag}} \sim 0.05$  compared to the same Hamiltonian on the triangular lattice. Thus, the phase boundary in Fig. 2 is finally corrected to,  $\mu = 3t + dE_{\text{mag}} + 6V_{\text{eff}}$ , showing excellent agreement with the ones obtained by the exact diagonalization.

*Remarks.*— The mechanism to generate a variety of phases in the spin-1/2 dimer model by the ring exchange interactions is fully fixed, by the exact transformation to a hard core bosonic language. We would like to stress the following points: The prototypes of emergent BEC's in spin systems were to dope magnons to a spin singlet state by the magnetic field, whereas, here, the ring exchange interaction serves as a *fictitious field that does not break the SU(2) symmetry*, and dopes the SU(2) bosons, not the magnons carrying magnetization. Once the bosons are doped, the bilinear-biquadratic interaction induced by a four-spin-exchange along the twisted path works to stabilize the nematic orders. The spin nematics basically requires an exchange of spin-1 bosons, thus was observed in the spin-1/2 system in a strong magnetic field (spin polarized state) or in the vicinity of frustrated magnetism, where the frustration played a key role to enhance the quantum fluctuation. Our spin singlet state is a trivial product state in the contour extreme limit of such a complication, thus one may feel it rather counterintuitive to have a nematic phase next to it.

The spin-1 hard core bosonic model can also be regarded as a strong coupling limit of the spinor boson systems studied in cold atoms. There, the bosons are softly exclusive on each site due to the on-site interaction,  $U$ ,<sup>49,50</sup> and the second order perturbation from the  $U/t \rightarrow \infty$  limit gives a biquadratic interaction between spin-1 bosons, and the nematic Mott insulating phase appears<sup>49–51</sup>. A situation similar to man-made optical lattices is naturally realized in our quantum spin-1/2 model representing crystalline solids, as such a dimer system is actually quite ubiquitous in transition metals such as  $\text{BaCuSi}_2\text{O}_6$ <sup>52</sup>,  $\text{Ba}_2\text{CoSi}_2\text{O}_6\text{Cl}_2$ <sup>53</sup>, and  $\text{Ba}_3\text{MRu}_2\text{O}_9$ <sup>54</sup>. In  $\text{Ba}_3\text{MRu}_2\text{O}_9$ , a nonmagnetic phase is actually found next to the singlet phase, and the relevance with our findings remains an issue to be clarified.

## ACKNOWLEDGMENTS

We thank Karlo Penc, Frédéric Mila, Shunji Tsuchiya, Ichiro Terasaki, and Katsuhiko Tanaka for discussions. This work is supported by JSPS KAKENHI Grant Numbers (No. JP17K05533, No.JP17K05497, and No.JP17H02916).

- \* chisa@phys.c.u-tokyo.ac.jp
- <sup>1</sup> P. Fazekas, P. W. Anderson, *Philos. Mag.* **30**, 423 (2006).
  - <sup>2</sup> P. W. Anderson, *Science* **235**, 1196 (1987).
  - <sup>3</sup> C. K. Majumdar, D. Ghosh, *J. Math. Phys.* **10**, 1388 (1969).
  - <sup>4</sup> A. F. Andreev, I. A. Grishchuk, *Sov. Phys. JETP* **60**, 267 (1984).
  - <sup>5</sup> N. Papanicolaou, *Nucl. Phys. B* **305**, 367 (1988).
  - <sup>6</sup> K. Harada, N. Kawashima, *Phys. Rev. B* **65**, 052403 (2002).
  - <sup>7</sup> B. Bauer, P. Corboz, A. M. Lauchli, L. Messio, K. Penc, M. Troyer, and F. Mila *Phys. Rev. B* **85**, 125116 (2012)
  - <sup>8</sup> Y. Oitmaa, C. J. Hamer, *Phys. Rev. B* **87**, 224431 (2013).
  - <sup>9</sup> I. Niesen, P. Corboz, *Phys. Rev. B* **95** 180404 (2017).
  - <sup>10</sup> I. Niesen, P. Corboz, *Sci. Post. Phys.* **3**, 030 (2017).
  - <sup>11</sup> H. Tsunetsugu and M. Arikawa, *J. Phys. Soc. Jpn.* **75**, 083701 (2006).
  - <sup>12</sup> A. Lauchli, F. Mila, and K. Penc, *Phys. Rev. Lett.* **97**, 087205 (2006).
  - <sup>13</sup> R. K. Kaul, *Phys. Rev. B* **86**, 104411 (2012)
  - <sup>14</sup> T. Momoi, P. Sindzingre, K. Kubo, *Phys. Rev. Lett.* **108**, 057206 (2012).
  - <sup>15</sup> N. Shannon, T. Momoi, and P. Sindzingre, *Phys. Rev. Lett.* **96**, 027213 (2006).
  - <sup>16</sup> H. Fukuyama, K. Yawata, T. Momoi, H. Ikegami, and H. Ishimoto, *arXiv/0505177v1* (2005).
  - <sup>17</sup> N. Nema, A. Yamaguchi, T. Hayakawa, and H. Ishimoto, *Phys. Rev. Lett.* **102**, 075301 (2009).
  - <sup>18</sup> A. Läuchli, J. C. Domenge, C. Lhuillier, P. Sindzingre, M. Troyer, *Phys. Rev. Lett.* **95**, 137206 (2005).
  - <sup>19</sup> G. Misguich, B. Bernu, C. Lhuillier, and C. Waldtmann, *Phys. Rev. Lett.* **81**, 1098 w (1998).
  - <sup>20</sup> G. Misguich, C. Lhuillier, B. Brnu, and C. Waldtmann, *Phys. Rev. B* **60**, 1064 (1999).
  - <sup>21</sup> W. LiMing, G. Misguich, P. Sindzingre, and C. Lhuillier, *Phys. Rev. B* **62**, 6372 (2000).
  - <sup>22</sup> H.-Y. Yang, A. M. Läuchli, F. Mila, K. Schmidt, *Phys. Rev. Lett.* **105**, 267204 (2010).
  - <sup>23</sup> H. Morita, S. Watanabe, and M. Imada, *J. Phys. Soc. Jpn.* **71**, 2109 (2002).
  - <sup>24</sup> Y. Shimizu, K. Miyagawa, K. Kanoda, M. Maesato, G. Saito, *Phys. Rev. Lett.* **91**, 107001 (2003).
  - <sup>25</sup> H. Katsura, N. Nagaosa, P. A. Lee, *Phys. Rev. Lett.* **104**, 066403 (2010).
  - <sup>26</sup> There is another term  $K_{R'}$ , comparable to  $K_R$  and  $K_T$  as shown in Ref.<sup>27</sup>, but plays an equivalent role with  $K_R$ , thus is abbreviated in the present paper.
  - <sup>27</sup> K. Tanaka, Y. Yokoyama, C. Hotta, *J. Phys. Soc. Jpn.* **87**, 023702 (2018).
  - <sup>28</sup> M. Takahashi, *J. Phys. C.* **10**, 1289 (1977).
  - <sup>29</sup> C. J. Calzado and J. P. Malrieu, *Phys. Rev. B* **69**, 094435 (2004).
  - <sup>30</sup> T. Giamarchi, A. M. Tsvelik, *Phys. Rev. B* **59**, 11398 (1999).
  - <sup>31</sup> T. Nikuni, M. Oshikawa, A. Oosawa, H. Tanaka, *Phys. Rev. Lett.* **84**, 5868 (2000).
  - <sup>32</sup> Ch. Rüegg, N. Cavadini, A. Furrer, H.-U. Gudel, K. Kramer, H. Mutka, A. Wildes, K. Habicht, P. Vorderwisch, *Nature* **423**, 62 (2003).
  - <sup>33</sup> M. Rice, *Science* **298** (2002) 760.
  - <sup>34</sup> A. V. Chubukov, *Phys. Rev. B* **43**, 3337 (1991).
  - <sup>35</sup> T. Hikiyama and S. Yamamoto, *J. Phys. Soc. Jpn.* **77**, 014709 (2008).
  - <sup>36</sup> Y. Yokoyama and C. Hotta, unpublished.
  - <sup>37</sup> S. Sachdev, R. N. Bhatt, *Phys. Rev. B* **41**, 9323 (1990).
  - <sup>38</sup> J.-D. Picon, A. F. Albuquerque, K. P. Schmidt, N. Laflorencie, M. Troyer, F. Mila, *Phys. Rev. B* **78**, 184418 (2008).
  - <sup>39</sup> P. W. Anderson, *Phys. Rev.* **86**, 694 (1952).
  - <sup>40</sup> B. Bernu, P. Lecheminant, C. Lhuillier, L. Pierre, *Phys. Rev. B* **50**, 10048 (1994).
  - <sup>41</sup> K. Penc, A. Läuchli, *Introduction to Frustrated Magnetism*, Chap.13, Springer, (2011).
  - <sup>42</sup> X.-F. Zhang, R. Dillenschneider, Y. Yu, S. Eggert, *Phys. Rev. B* **84**, 174515 (2011).
  - <sup>43</sup> See the Supplementary Material. The accuracy of the phase diagram of the hard core bosonic model at  $t < 0$  is provided therein.
  - <sup>44</sup> S. Wessel, M. Troyer, *Phys. Rev. Lett.* **95**, 127205 (2005).
  - <sup>45</sup> D. Heidarian, K. Damle, *Phys. Rev. Lett.* **95**, 127206 (2005).
  - <sup>46</sup> R. G. Melko, A. Paramekanti, A. A. Burkov, A. Vishwanath, D. N. Sheng, L. Balents, *Phys. Rev. Lett.* **95**, 127207 (2005).
  - <sup>47</sup> A. A. Burkov, L. Balents, *Phys. Rev. B* **72**, 134502 (2005).
  - <sup>48</sup> The dip is not the finite size effect or the artifact of choosing particular cluster shape. Details are provided in the Supplemental Material.
  - <sup>49</sup> T. Kimura, Sh. Tsuchiya and S. Kurihara, *Phys. Rev. Lett.* **94**, 110403 (2005).
  - <sup>50</sup> L. de F. de Parny, H. Yang, F. Mila, *Phys. Rev. Lett.* **113**, 200402 (2014).
  - <sup>51</sup> L. de F. de Parny, F. Hebert, V. G. Rousseau, G. G. Batrouni, *Phys. Rev. B* **88**, 104509 (2013).
  - <sup>52</sup> S. E. Sebastian, N. Harrison, C. D. Batista, L. Balicas, M. Jaime, P. A. Sharma, N. Kawashima, I. R. Fisher, *Nature*, **441**, 617 (2006).
  - <sup>53</sup> H. Tanaka, N. Kurita, M. Okada, E. Kunihiro, Y. Shirata, K. Fujii, H. Uekusa, A. Matsuo, K. Kindo, H. Nojiri, *J. Phys. Soc. Jpn.* **83**, 103701 (2014).
  - <sup>54</sup> I. Terasaki, T. Igarashi, T. Nagai, K. Tanabe, H. Taniguchi, T. Matsushita, N. Wada, A. Takata, T. Kida, M. Hagiwara, K. Kobayashi, H. Sagayama, R. Kumai, H. Nakao, Y. Murakami *J. Phys. Soc. Jpn.* **86** (2017), 033702.